Water Research 254 (2024) 121372

Contents lists available at ScienceDirect

Water Research

journal homepage: www.elsevier.com/locate/watres

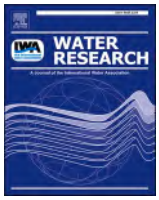

Assessing ammonium pollution and mitigation measures through a modified watershed non-point source model

Feng Han [a], Qing Tian [b], Nengwang Chen [b,*], Zhaoping Hu [a], Yao Wang [b], Rui Xiong [a,c], Peng Xu [a], Wei Liu [a], Alejandra Stehr [d], Ricardo O. Barra [e], Yi Zheng [a,c,f]

[a] School of Environmental Science and Engineering, Southern University of Science and Technology, Shenzhen 518055, China
[b] Fujian Provincial Key Laboratory for Coastal Ecology and Environmental Studies, College of the Environment and Ecology, Xiamen University, Xiamen 361102, China
[c] Shenzhen Municipal Engineering Lab of Environmental IoT Technologies, Southern University of Science and Technology, Shenzhen 518055, China
[d] Faculty of Engineering, University of Concepción, 4070386 Concepción, Chile
[e] Faculty of Environmental Sciences and EULA Chile Centre, University of Concepción, 4070386 Concepción, Chile
[f] State Environmental Protection Key Laboratory of Integrated Surface Water-Groundwater Pollution Control, Southern University of Science and Technology, Shenzhen 518055, China

ARTICLE INFO

Keywords:
Ammonium nitrogen
Non-point source pollution
SWAT model
Mitigation measures
Source-contribution analysis
Jiulong River Watershed

ABSTRACT

Watershed water quality modeling is a valuable tool for managing ammonium (NH_4^+) pollution. However, simulating NH_4^+ pollution presents unique challenges due to the inherent instability of NH_4^+ in natural environment. This study modified the widely-used Soil and Water Assessment Tool (SWAT) model to simulate non-point source (NPS) NH_4^+ processes, specifically incorporating the simulation of land-to-water NH_4^+ delivery. The Jiulong River Watershed (JRW) is the study area, a coastal watershed in Southeast China with substantial sewage discharge, livestock farming, and fertilizer application. The results demonstrate that the modified model can effectively simulate the NPS NH_4^+ processes. It is recommended to use multiple sets of observations to calibrate NH_4^+ simulation to enhance model reliability. Despite constituting a minor proportion (5.6 %), point source inputs significantly contribute to NH_4^+ load at watershed outlet (32.4~51.9 %), while NPS inputs contribute 15.3~17.3 % of NH_4^+ loads. NH_4^+ primarily enters water through surface runoff and lateral flow, with negligible leaching. Average NH_4^+ land-to-water delivery rate is about 2.35 to 2.90 kg N/ha/a. High delivery rates mainly occur at agricultural areas. Notably, proposed NH_4^+ mitigation measures, including urban sewage treatment enhancement, livestock manure management improvement, and fertilizer application reduction, demonstrate potential to collectively reduce the NH_4^+ load at watershed outlet by 1/4 to 1/3 and significantly enhance water quality standard compliance frequency. Insights gained from modeling experience in the JRW offer valuable implications for NH_4^+ modeling and management in regions with similar climates and significant anthropogenic nitrogen inputs.

1. Introduction

Ammonium (NH_4^+) is a common toxicant form of nitrogen in soils and water bodies. The term NH_4^+ refers to both the ionized and un-ionized states (ammonia, NH_3) in this study. NH_4^+ plays a crucial role in the terrestrial nitrogen cycle. In soils, NH_4^+ can be taken up by plants, oxidized to nitrate (NO_3^-), volatilized into air as NH_3, or transported into rivers or lakes via surface runoff. In aquatic environment, NH_4^+ is often a preferred source of nitrogen for aquatic organism (Zhou et al., 2017). Elevated NH_4^+ concentrations can lead to water quality deterioration and stimulate the growth of algae and aquatic plants, potentially contributing to eutrophication Ding et al. (2022). Accordingly, NH_4^+ is often used as an indicator for the surface water quality assessment (Zaidi Farouk et al. 2023). Over the past few decades, global emissions of reactive nitrogen (of which NH_4^+ is one major form) have steadily increased (Zhang et al., 2021), which has exacerbated nitrogen pollution in rivers, lakes, and coastal waters (Gu et al., 2023). Xu et al. (2024) estimated the global NH_3 gas emissions from rice, wheat, and maize fields in 2018 to be 4.3 Tg N/a, accounting for 3.6 % of chemical fertilizer usage (120 Tg N/a) (Gu et al., 2023). Nevertheless, accurate estimates of NH_4^+ released from land to water on a global scale are currently lacking. China also faces a severe issue of nitrogen pollution in

* Corresponding author at: College of the Environment and Ecology, Xiamen University, Xiamen 361102, Fujian Province, China.
E-mail address: nwchen@xmu.edu.cn (N. Chen).

https://doi.org/10.1016/j.watres.2024.121372
Received 16 November 2023; Received in revised form 7 February 2024; Accepted 23 February 2024
Available online 23 February 2024

its water bodies (Yu et al., 2019). Despite China's efforts to control NH_4^+ pollution, achieving complete control of NH_4^+ for attaining a good ecological status requires a significant amount of time (Zhang et al., 2023).

NH_4^+ may originate from various sources. In China, NH_4^+ primarily originates from domestic sewage discharge (73 %), livestock farming (12 %), and fertilizer application (9 %) (MEE 2020). Among these three sources, domestic sewage is a typical point source (PS) pollution, fertilizers are non-point source (NPS) pollution, and livestock manures can be either PS pollution or NPS pollution. To understand the linkage between these sources and their water quality impacts, it is crucial to comprehend the transport and biogeochemical processes of NH_4^+ within the watershed. In this context, watershed water quality (WWQ) models that offer quantitative, spatially-distributed, and process-based information are valuable tools (Wellen et al., 2015). WWQ models typically encompass the simulation of pollutant generation, land-to-water delivery, and in-stream processes (Fu et al., 2019). Presently, there are dozens of WWQ models documented in the literature, among which some widely used models include Soil and Water Assessment Tool (SWAT) (Neitsch et al., 2011), Hydrological Simulation Program-FORTRAN (HSPF) (Bicknell et al., 1997), Annualized AGricultural Non-Point Source pollution model (AnnAGNPS) (Bingner et al., 2018), SPAtially Referenced Regression On Watershed attributes (SPARROW) (Schwarz et al., 2006) and Integrated Catchment Model (INCA) (Wade et al., 2002).

SWAT is the most widely used model (Fu et al., 2019). SWAT's popularity is primarily due to its comprehensive functionality and reliable results. It can simulate a wide range of hydrological processes, soil erosion, sediment transport, nutrient cycling, plant growth, as well as various agricultural and water management practices (Neitsch et al., 2011). In terms of NH_4^+ simulation, SWAT considers multiple NH_4^+ inputs, including atmospheric deposition, fertilization, and PS discharges. It also simulates NH_4^+ nitrification and NH_3 volatilization in soil and in-stream NH_4^+ transport and transformation. However, in the SWAT model, NH_4^+ is considered immobile in soil, resulting in a lack of land-to-water delivery simulation, which is crucial for addressing NPS NH_4^+ pollution. One main reason for this limitation is the strong retention of NH_4^+ by soils. Nevertheless, observational studies have reported that NH_4^+ can be flushed or transported into receiving water bodies via surface runoff and lateral flow (Ao et al., 2020; Daniels et al., 2012; O'Mara et al., 2019; Xing et al., 2023). Considering the low mobility of NH_4^+ and its inherent instability (easily oxidize into NO_3^-), such simplification is acceptable when the focus is on NO_3^- simulation. However, given the significance of NH_4^+ in water quality management and the substantial worldwide SWAT community, some enhancements to the NH_4^+ simulation in SWAT are considered necessary.

There have been several studies in the literature that utilize WWQ models to simulate NH_4^+ pollution. Some popular models include HSPF, INCA, SPARROW, and SWAT. For instance, Zhu et al. (2023) employed HSPF to simulate nitrogen pollution (including NH_4^+) in a coastal watershed in North America. Nevertheless, HSPF does not comprehensively depict in-stream water quality processes, so the authors integrated HSPF with the Water Quality Analysis Simulation Program (WASP) in their study. Moreover, HSPF lacks a plant growth module, thus it cannot depict the intricate interaction between crop growth and soil nutrient cycle. Vaighan et al. (2019) used INCA to simulate the impacts of climate and land use changes on NH_4^+ pollution in the Kor River Basin, Iran. INCA has a simple model structure and simulates the dynamics of NH_4^+ in soils and rivers by solving a series of differential equations. INCA does not simulate plant growth processes, too. Dai et al. (2021) used the SPARROW model to simulate the sources and transport of NH_4^+ in a karst watershed in China. Compared to mechanistic models like SWAT, SPARROW is primarily a statistical model, which limits its applicability in terms of process understanding. Jiang et al. (2023) used SWAT to simulate NH_4^+ pollution in the Dongjiang River Watershed in China. However, they utilized the original SWAT model, which does not simulate the land-to-water delivery of NH_4^+. The NPS NH_4^+ pollution in their study is indirectly represented through the NPS pollution of organic nitrogen (orgN), which is hydrolyzed into NH_4^+ in the water.

In this study, we modified the SWAT model by enabling the simulation of NH_4^+ movement in soils and the land-to-water delivery. This modification can potentially expand the applications of SWAT in the context of NH_4^+ simulation, NH_4^+ management, and agriculture-water quality nexus issues. Using the modified model, we simulated NH_4^+ pollution in the Jiulong River Watershed (JRW), a coastal watershed in Southeast China. The JRW is characterized by notable sewage discharge, substantial livestock farming, and significant fertilizer application, which aligns closely with the sources of NH_4^+ pollution in China. It serves as an ideal study area for researching NH_4^+ pollution and its modeling methods. We comprehensively considered the specific sources of NH_4^+ pollution in the watershed, including atmospheric deposition, domestic sewage, livestock farming, fertilizer application, and industrial discharges. The model was calibrated against multiple sets of observational data using an advanced optimization algorithm, DYnamic COordinate search using Response Surface models (DYCORS) (Regis and Shoemaker 2013). With the calibrated model, we examined the features of NH_4^+ pollution originating from various land uses and quantified the contributions of PS and NPS inputs to NH_4^+ load at watershed outlet. Based on the source-contribution analysis, we proposed three NH_4^+ pollution mitigation measures and evaluated their effectiveness in improving water quality. The insights gained from the JRW can serve as valuable references for watershed-scale NH_4^+ simulations and the development of mitigation strategies in other areas.

2. Materials and methods

2.1. SWAT model modification

2.1.1. SWAT model description

The SWAT model is developed by USDA Agricultural Research Service and Texas A&M AgriLife Research (Neitsch et al., 2011). In SWAT, a watershed is divided into a number of subbasins, and each subbasin is further divided into multiple hydrological response units (HRUs). Each HRU exhibits homogeneous land use, soil, and slope conditions. The river network is segmented into multiple reaches, where each subbasin contains one reach. During daily simulations, the SWAT model initially performs land phase simulation and delivers the water and pollutants generated from HRUs to respective reaches. Subsequently, the water and pollutants are routed downstream through the river network to the watershed outlet.

The SWAT model specifically simulates the nitrogen cycle in soils due to its fundamental importance and critical role in plant growth. Within the model, five nitrogen forms are considered: two inorganic forms (i.e., NO_3^- and NH_4^+) and three organic forms. As depicted in Fig. 1, orgN and NH_4^+ can be transformed into NO_3^- via mineralization and nitrification, respectively. NO_3^- can be removed from soil by plant uptake and denitrification. NH_4^+ can be lost through nitrification and NH_3 volatilization. Due to the anionic nature, NO_3^- is very susceptible to move in soils. SWAT simulates the transport of NO_3^- in surface runoff and lateral flow, as well as its leaching into groundwater. Conversely, in SWAT, NH_4^+ is assumed to be adsorbed by soils and is not permitted to move. For a comprehensive understanding of these processes, please refer to the theoretical documentation (Neitsch et al., 2011).

2.1.2. Modifications of SWAT to enhance NH_4^+ simulation

The modifications include altering the mineralization product of orgN from NO_3^- to NH_4^+, simulating NH_4^+ movement with runoff and lateral flow, simulating the leaching process, and modeling NH_4^+ transport in groundwater (Fig. 1). The first modification is undertaken because NH_4^+, rather than NO_3^-, is the immediate product of orgN mineralization (Schimel and Bennett 2004). For example, orgN is mineralized to NH_4^+ in DNDC (UNH-ISEOS 2017) and DayCent

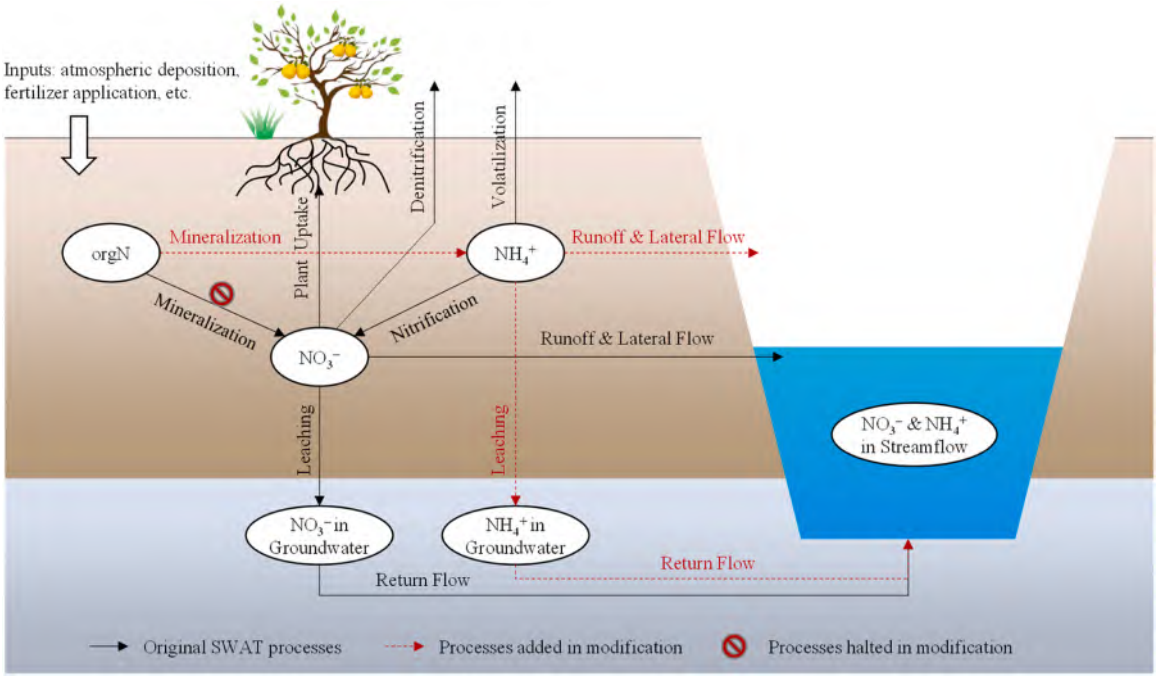

Fig. 1. Schematic overview of the nitrogen cycle processes in the original and modified SWAT model. NO_3^-, NH_4^+ and orgN represent nitrate, ammonium, and organic nitrogen, respectively.

(Delgrosso et al., 2005), which are two classic biogeochemical models. The mathematical methods for other three modifications are provided as follows.

In soils, NH_4^+ exists in either an aqueous phase or an adsorption phase. The equilibrium between the two phases is described by a partition coefficient, K_{NH4} (L/kg). Aqueous NH_4^+ can be transported with surface runoff, lateral flow, and percolation water. The concentration of aqueous NH_4^+ in mobile soil water [c_{NH4}, kg N/(ha·mm H_2O)] is determined as follows:

$$c_{NH4} = \frac{NH4_{tot}}{w_{mobile}}\left[1 - \exp\left(\frac{-w_{mobile}}{SAT + K_{NH4}\cdot\rho_b\cdot thk}\right)\right] \quad (1)$$

where $NH4_{tot}$ is NH_4^+ amount in a soil layer (kg N/ha), w_{mobile} is mobile water (mm H_2O), SAT is water amount at saturation (mm H_2O), ρ_b is the bulk density (g/cm^3), and thk is soil thickness (mm). The derivation of Eq. (1) is provided in Text S1 in the Supplementary Materials (SM).

Then, the NH_4^+ transported with surface runoff, lateral flow, and percolation water, namely, $NH4_{surf}$, $NH4_{lat}$ and $NH4_{perc}$ (kg N/ha), can be calculated as follows:

$$NH4_{surf} = Q_{surf}\cdot c_{NH4}\cdot\beta_1 \quad (2)$$

$$NH4_{lat} = \begin{cases} Q_{lat}\cdot c_{NH4}\cdot\beta_1 \text{ for the 1st layer} \\ Q_{lat}\cdot c_{NH4}\cdot\beta_2 \text{ for lower layers} \end{cases} \quad (3)$$

$$NH4_{perc} = w_{perc}\cdot c_{NH4} \quad (4)$$

where Q_{surf} is surface runoff (mm H_2O), Q_{lat} is lateral flow (mm H_2O), and w_{perc} is percolation water (mm H_2O), and β_1 and β_2 are two adjustment coefficients. β_1 and β_2 can be determined through model calibration.

NH_4^+ adsorbed to soil particles can be eroded and transported to reaches by surface runoff. The amount of eroded NH_4^+, $NH4_{sed}$ (kg N/ha), is calculated as follows:

$$NH4_{sed} = 0.001\cdot\frac{sed}{A}\cdot c_{soild}\cdot\varepsilon_r \quad (5)$$

where sed is sediment yield (t), A is HRU area (ha), c_{soild} is concentration of adsorbed NH_4^+ in top layer (mg N/kg soil), and ε_r is the enrichment ratio.

NH_4^+ that leaches out of the soil zone (i.e., $NH4_{perc}$ for the bottom layer) will move with percolation water through the vadose zone and enter shallow groundwater. The exponential decay weighting function, utilized to account for the time delay in NO_3^- leaching from soil zone to groundwater, is also employed to account for the delay in NH_4^+ transport:

$$NH4_{rchrg,i} = [1 - \exp(-1/\delta_{NH4})]\cdot NH4_{perc} + \exp(-1/\delta_{NH4})\cdot NH4_{rchrg,i-1} \quad (6)$$

where $NH4_{rchrg,i}$ is the amount of NH_4^+ entering groundwater on day i (kg N/ha), and δ_{NH4} is the delay time in NH_4^+ transport (d). In SWAT, the delay time for NO_3^- (δ_{NO3}) is equal to the delay time for percolation water (δ_{gw}). This assumption is not applicable for NH_4^+. According to Böhlke et al. (2006), NH_4^+ moves at a rate about 0.25 times the groundwater velocity. In this study, δ_{NH4} is assumed to be δ_{gw}/r_{NH4}, where r_{NH4} is an adjustment coefficient with a default value of 0.25.

The nitrification of NH_4^+ in the vadose zone is considered as follows:

$$NH4_{nit,unsat,i} = F_{nit,unsat}\cdot NH4_{unsat,i} \quad (7)$$

$$NH4_{unsat,i} = \frac{\exp(-1/\delta_{NH4})}{1 - \exp(-1/\delta_{NH4})}\cdot NH4_{rchrg,i} \quad (8)$$

where $NH4_{nit,unsat,i}$ is the NH_4^+ nitrified in the vadose zone on day i (kg N/ha), $F_{nit,unsat}$ is the nitrification rate in the vadose zone (1/d), and $NH4_{unsat,i}$ is the amount of NH_4^+ stored in the vadose zone (kg N/ha). The calculated $NH4_{nit,unsat,i}$ will be subtracted from $NH4_{unsat,i}$ and added to the NO_3^- storage in the vadose zone. Consequently, the amount of NH_4^+ and NO_3^- entering groundwater for the following day will be proportionally adjusted.

Similar to NO_3^-, NH_4^+ in the shallow aquifer can either remain in the aquifer, be transported to deep aquifer (GW_{seep}), or move with groundwater flow into the reaches (GW_q). The calculation methods for NH_4^+ movements are similar to the methods used for NO_3^-. The key distinction

lies in that NH_4^+ concentrations in GW_{seep} and GW_q are r_{NH4} times the NH_4^+ concentration in groundwater. This adjustment accounts for the retardation effect of NH_4^+ transport in groundwater. The nitrification of NH_4^+ in groundwater is considered similar to Eq. (7), introducing a parameter, $F_{nit,sat}$ (1/d).

2.2. Study area

The JRW is in Fujian province, China (Fig. 2a), spanning an area of ~14,700 km^2. The Jiulong River comprises two main tributaries, North River and West River (Fig. 2b). The two tributaries converge near the estuary and discharge into Xiamen Bay. The North River Watershed (NRW) and West River Watershed (WRW) cover areas of 9640 km^2 and 3940 km^2, respectively. The JRW experiences a subtropical monsoon climate, characterized by hot and rainy summers, and warm and humid winters. The annual precipitation is 1656 mm, and the average temperature is 22 °C. The topography in the JRW is mostly hilly. Most mountain areas are covered by natural forests. According to the 2018 land use map, the JRW is characterized by 71.8 % forest, 7.8 % cropland, 7.6 % orchard, 6.7 % urban or built-up area, 3.3 % tea garden, and 2.8 % other land use types (e.g., grassland, bareland, water). The cropland primarily cultivates rice, corn, peanuts, and vegetables, while the orchard mainly grows pomelos, lychees, and bananas.

Nitrogen pollution, especially NH_4^+, is a major environmental concern in the JRW due to rapid economic development, urbanization, and population growth in the region (Fig. S1a in the SM). The Gross Domestic Product (GDP) of the 10 counties/districts/county-level cities (referred to as "counties" hereafter) within the JRW was below 50 billion Chinese Yuan (CNY) in 2000. By 2019, it was approximately 500 billion CNY. Fertilizer application (Fig. S1b in the SM) and livestock farming (Fig. S1c in the SM) also increased significantly since 1980. The surge in anthropogenic nitrogen inputs has led to excessive nitrogen released into Xiamen Bay, which now faces a serious threat of eutrophication (Chen et al., 2021; Luo et al., 2022). Despite years of dedicated efforts to address nutrient pollution, nitrogen pollution remains a persistent challenge in the JRW (Kong et al., 2015). Exploring effective management strategies for nitrogen reduction is crucial for ensuring the long-term green development of the JRW.

2.3. Simulating nitrogen pollution in the JRW

2.3.1. Data description

Table S1 in the SM lists the data used for establishing, calibrating, and validating the model. The digital elevation model (DEM) and river network map were used to delineate the watershed. The land use and soil data were used to define and parameterize HRUs, where soil texture data has been transformed from the Chinese standard to the U.S. standard using the SPAW model (Saxton and Willey, 2005). Meteorological data from 10 weather stations were used to force the model. Atmospheric nitrogen deposition data were collected to determine the rates of dry and wet deposition of NO_3^- and NH_4^+.

In August 2020, we conducted a field survey on crop management practices within the JRW and obtained 86 valid questionnaires. Through this survey, the fertilizer application rate for each crop type was determined (Fig. S2 in the SM). We also collected JRW's annual data on nitrogen fertilizer application, livestock farming, population and GDP from local statistical yearbooks, as well as PS discharge data from China's Second National Census of Pollution Sources (MEE 2020). These data were used to determine the crop management practices, especially fertilizer application, and PS discharges in the SWAT model. Additionally, streamflow observations at 2 stations (PN and ZD in Fig. 2c), sediment observations at 2 stations (PN and ZD in Fig. 2c), and nitrogen

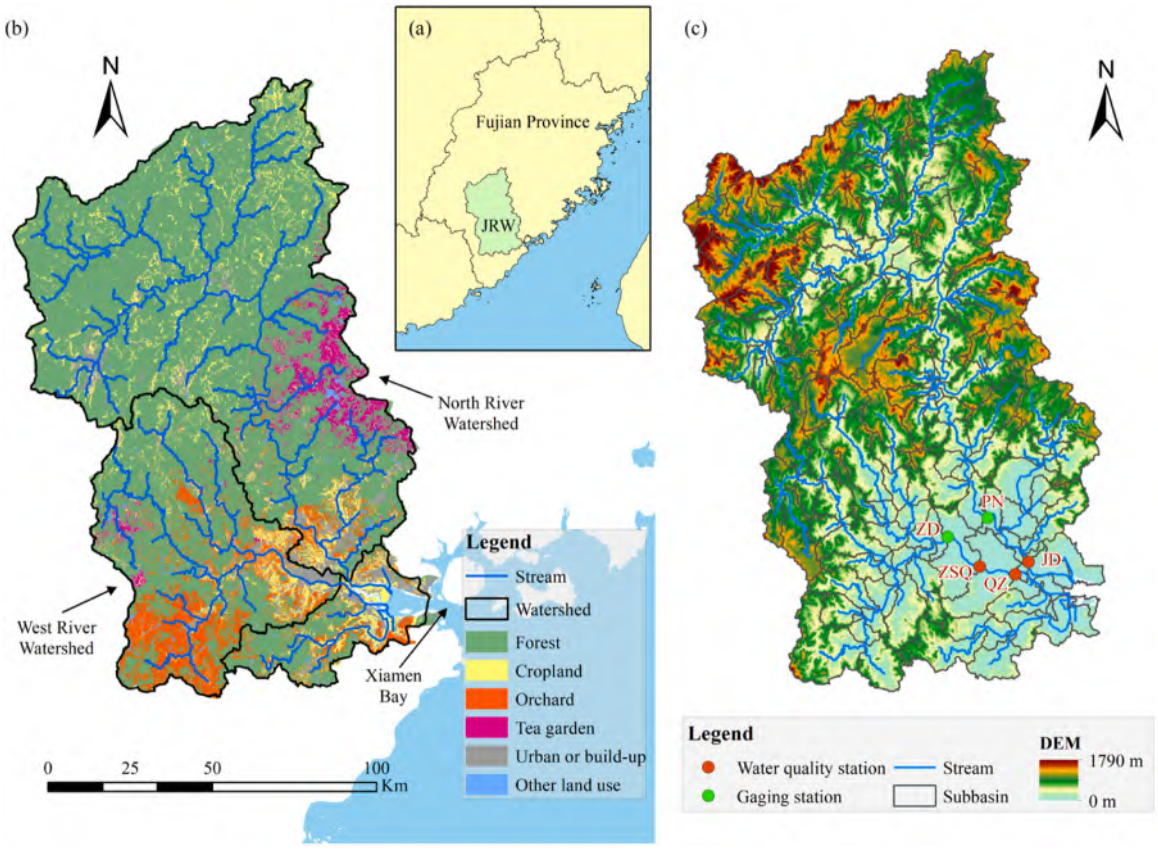

Fig. 2. Overview of the Jiulong River Watershed (JRW). (a) Location, (b) land use, and (c) watershed delineation. Punan (PN) and Jiangdong (JD) stations are to observe North River, while Zhengdian (ZD), Zhongshanqiao (ZSQ) and Qiaozha (QZ) stations are to observe West River.

observations (both NO_3^- and NH_4^+) at 3 stations (JD, ZSQ and QZ in Fig. 2c) were collected or monitored to calibrate and validate the model.

To accurately simulate nitrogen pollution within the JRW, we quantitatively assessed the anthropogenic nitrogen inputs over the past 20 years (2000–2019). These inputs encompass urban domestic sewage, rural domestic sewage, manure generated from livestock farming, industrial wastewater, and chemical fertilizer application. The assessment was conducted at the county level and on an annual basis. The detailed description of the assessment methods for these inputs was provided in Text S2 in the SM.

2.3.2. Model setup

The watershed was discretized into 168 subbasins (Fig. 2c) and 1828 HRUs. The simulation period is from 2000 to 2019, with the first 2 years being the warm-up period. The model configuration for nitrogen simulation primarily involves three components: atmospheric nitrogen deposition, agricultural management practices (especially fertilization), and PS discharges. Nitrogen deposition rates for each subbasin and year were determined using the nitrogen deposition dataset in China (Jia et al., 2019, 2021). In the JRW, the average deposition flux for NH_4^+ and NO_3^- is 15.83 and 11.09 kg N/ha/a, respectively. The scheduled management practices for each crop type were determined based on the field survey, and the fertilization rate in a certain year was adjusted according to the estimated nitrogen input for that year (Text S2 in the SM). In addition to chemical fertilizer, cropland also receives rural domestic sewage (i.e., $N_{rur,2}$), and manure from livestock farming (i.e., *M1*) (Text S2 in the SM). $N_{rur,2}$ and *M1* were estimated at the county level, and they were evenly distributed to all cropland within the county. The PS discharges comprises urban domestic sewage (i.e., $N_{urb,1}$ and $N_{urb,2}$), rural domestic sewage (i.e., $N_{rur,1}$), manure from livestock farming (i.e., *M2* and *M3*), and industrial wastewater (e.g., $NH4_{ind,ij}$) (Text S2 in the SM). $N_{urb,1}$, $N_{urb,2}$, $N_{rur,1}$, *M2*, and *M3* were also estimated at the county level. $N_{urb,1}$ and $N_{urb,2}$ in a county was allocated to the subbasin where the central urban area of that county is located, $N_{rur,1}$ was distributed among the subbasins in that county based on residential area, and *M2* and *M3* were distributed among the subbasins based on cropland area. Industrial wastewater was directly assigned to the subbasin where the factory is located.

2.3.3. Sensitivity analysis, model calibration and validation

Before model calibration, 43 parameters affecting the simulation of streamflow, sediment, NO_3^-, and NH_4^+ were initially selected from hundreds of SWAT parameters (Table S2 in the SM). The key parameter for NH_4^+ transport simulation, K_{NH4}, was included, with a specified range of 0.5~8 L/kg. This range refers to the laboratory investigation by the Environment Agency in England (EA 2005). Additionally, a fertilization rate adjustment factor (FRT_ADJ) and a PS load adjustment factor (PS_ADJ) were introduced to account for uncertainties in estimating anthropogenic nitrogen inputs. The aggregate parameter method (Yang et al., 2007) was employed to adjust the parameter values: varying the parameter value directly (type I); adding a deviation to the prior parameter (type II); and applying a multiplier to the prior parameter (type III). The Morris method (Campolongo et al., 2007; Morris 1991) was employed to select sensitive parameters. Text S3 in the SM provides a brief introduction of the algorithm and the parameter configuration in this study. Ultimately, we identified 13 streamflow-sensitive parameters ($\boldsymbol{\theta}_H$), 5 sediment-sensitive parameters ($\boldsymbol{\theta}_S$) and 12 nitrogen-sensitive parameters ($\boldsymbol{\theta}_N$). Table S3 in the SM lists the selected sensitive parameters.

In this study, a stepwise calibration approach was applied to parameterize the model. The NRW and WRW were calibrated individually due to notable differences in topography, hydrological conditions, and pollution patterns between the two watersheds. During the calibration process, the simulation results of streamflow, sediment and nitrogen were evaluated as follows:

$$f_H = -NSE(\mathbf{Y}_H, \mathbf{Z}_H) \tag{9}$$

$$f_S = -NSE(\mathbf{Y}_S, \mathbf{Z}_S) + |PBIAS(\mathbf{Y}_S, \mathbf{Z}_S)/100| \tag{10}$$

$$\begin{aligned} f_N = &-NSE(\mathbf{Y}_{NH4}, \mathbf{Z}_{NH4}) + |PBIAS(\mathbf{Y}_{NH4}, \mathbf{Z}_{NH4})/100| \\ &-NSE(\mathbf{Y}_{NO3}, \mathbf{Z}_{NO3}) + |PBIAS(\mathbf{Y}_{NO3}, \mathbf{Z}_{NO3})/100| \end{aligned} \tag{11}$$

where **Y** represents the simulation results, **Z** represents the observations, subscripts H, S and N (NH_4 and NO_3) respectively denote streamflow, sediment, and nitrogen (NH_4^+ and NO_3^-), NSE represents the Nash–Sutcliffe Efficiency coefficient, and PBIAS represents Percent Bias. The evaluation functions for sediment and nitrogen were designed this way because of the inherent higher uncertainty in water quality modeling, making it impractical to achieve very high NSE values. Excessively focusing on high NSE values may lead to adverse effects, such as notable simulation bias. By introducing an error metric (e.g., PBIAS), the composite metric not only assesses the model's daily performance but also evaluates overall error. This practice, i.e., aggregating multiple evaluation indices into a single metric, has been commonly employed to seek more coherent calibration results (Althoff and Rodrigues 2021).

As illustrated in Fig. S3 in the SM, the first step is to calibrate streamflow simulation. In this step, $\boldsymbol{\theta}_S$ and $\boldsymbol{\theta}_N$ were fixed at default values (i.e., $\boldsymbol{\theta}_{S,0}$ and $\boldsymbol{\theta}_{N,0}$), while $\boldsymbol{\theta}_H$ was optimized by DYCORS, with the objective being to minimize f_H. The second step is to calibrate sediment simulation. In this step, $\boldsymbol{\theta}_H$ took the calibrated values ($\boldsymbol{\theta}_{H,C}$), $\boldsymbol{\theta}_N$ were fixed at default values, and $\boldsymbol{\theta}_S$ was optimized, with the objective being to minimize $f_H + f_S$. In this step, f_H was also included in the objective to ensure that the sediment simulation calibration does not significantly deteriorate the streamflow simulation. The last step is to calibrate NH_4^+ and NO_3^- simulation. In this step, $\boldsymbol{\theta}_H$ and $\boldsymbol{\theta}_S$ took their calibrated values (i.e., $\boldsymbol{\theta}_{H,C}$ and $\boldsymbol{\theta}_{S,C}$), and $\boldsymbol{\theta}_N$ was optimized, with the objective being to minimize $f_H + f_S + f_N$. Details of the data, stations, and periods for model calibration and validation are presented in Table S4 in the SM.

2.4. Simulation scenarios

An important goal of this study is to assess the contributions of various NH_4^+ inputs to the NH_4^+ load at watershed outlet, with a specific focus on NPS inputs. To achieve this goal, we designed several simulation scenarios. Here, the model described in Section 2.3 is considered as the baseline scenario, denoted as S0. Based on Scenario S0, we designed three simulation scenarios: S1, removing PS NH_4^+ inputs and not simulating the NPS processes of NH_4^+; S2, with PS NH_4^+ inputs and not simulating the NPS processes of NH_4^+; and S3, removing PS NH_4^+ inputs and simulating the NPS processes of NH_4^+. All other model settings remain the same as Scenario S0.

Based on the results of source-contribution analysis (Section 3.2.3), we proposed three potentially effective measures for mitigating NH_4^+ pollution in the JRW, namely, enhancing urban sewage treatment, improving livestock manure management, and reducing application of chemical fertilizers. Specifically, enhancing urban sewage treatment involves setting the minimum sewage collection rate to 0.9 ($R_{urb,1}$ in Eq. S10 in the SM) and setting the minimum nitrogen removal efficiency to 0.7 ($R_{urb,2}$ in Eq. S10 in the SM). Improving livestock manure management refers to collecting and treating manure that was previously discharged into rivers (i.e., changing *M3* to *M2*). As for the third measure, we consider a 30 % reduction in fertilization rates. The details and rationale for these measures have been outlined in Text S4 in the SM. By implementing these measures individually or collectively, four simulation scenarios were designed, denoted as S4-S7. All other model settings remain the same as Scenario S0.

3. Results

3.1. Model calibration and validation

Fig. 3 presents the observed and simulated streamflow, sediment, NH_4^+, and NO_3^- during calibration and validation periods. Corresponding evaluation metric values are listed in Table 1. As depicted in Fig. 3a and b, the SWAT model successfully reproduced the daily streamflow in both the NRW and WRW. The NSE values for both watersheds during calibration and validation periods are around 0.80, indicating an excellent model performance. The model also works well in sediment simulation. As illustrated in Fig. 3c and d, the model can reasonably predict sediment concentrations during both flood periods (high values) and baseflow periods (low values). The NSE values for daily sediment simulation during both calibration and validation periods range from 0.27 to 0.45, which can be considered satisfactory from a water quality modeling perspective (Moriasi et al., 2007).

Simulation results of NH_4^+ and NO_3^- are acceptable. The simulation

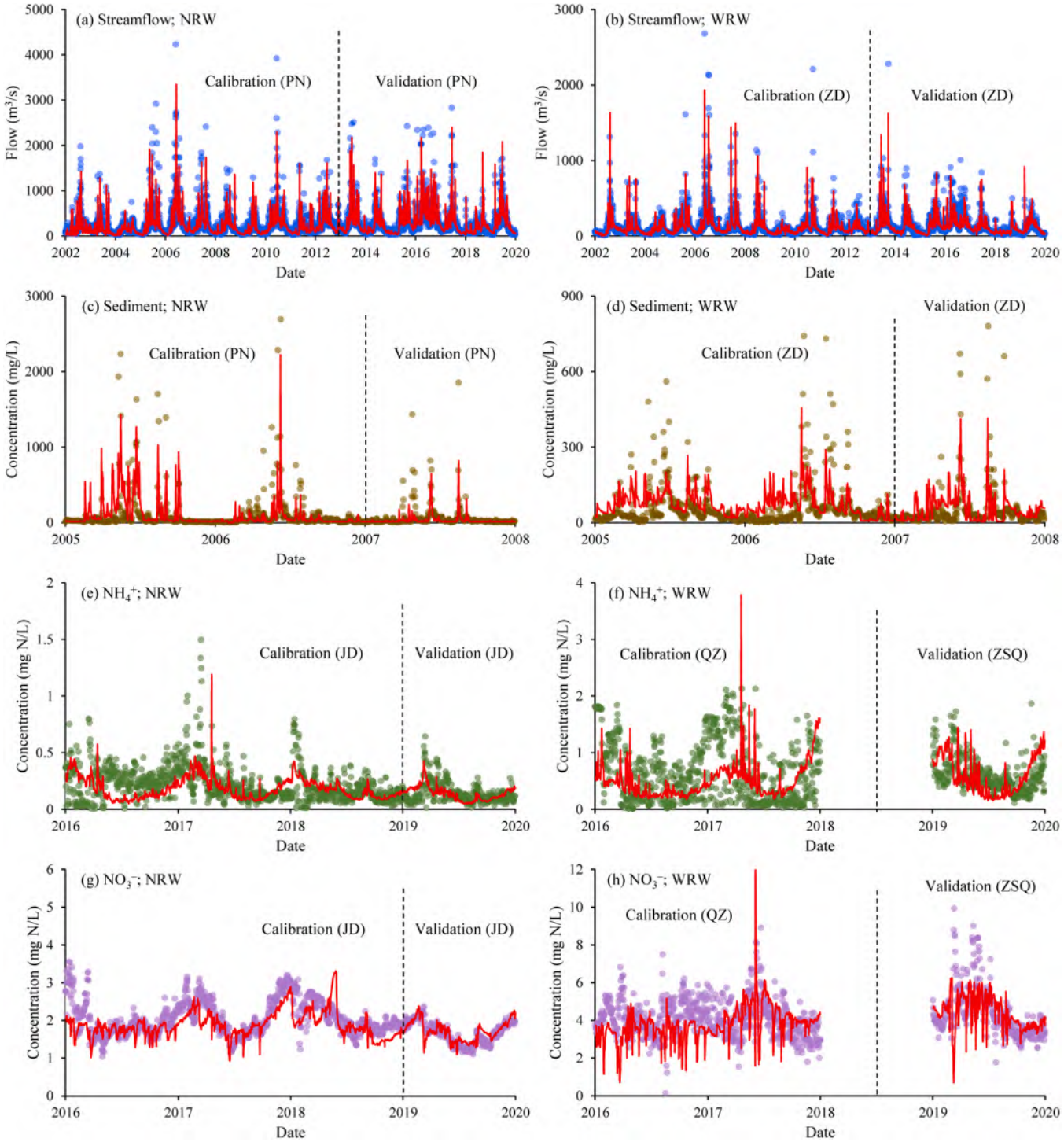

Fig. 3. Comparison of observed and simulated streamflow, sediment, ammonium (NH_4^+), and nitrate (NO_3^-) in both North River Watershed (NRW) and West River Watershed (WRW) during calibration and validation periods at Punan (PN), Zhengdian (ZD), Jiangdong (JD), Qiaozha (QZ), and Zhongshanqiao (ZSQ) stations. Dots represent observations, while red lines represent simulation results.

Table 1
SWAT model performance in the Jiulong River Watershed.

	Model response	Calibration		Validation	
		NSE	PBIAS	NSE	PBIAS
North River Watershed	Streamflow	0.79	\	0.78	\
	Sediment	0.31	5.4 %	0.45	−40.6 %
	NH_4^+	0.00	−15.5 %	0.20	0.1 %
	NO_3^-	0.14	−8.0 %	0.49	3.2 %
West River Watershed	Streamflow	0.81	\	0.76	\
	Sediment	0.27	10.1 %	0.39	4.4 %
	NH_4^+	−0.13	−23.1 %	−0.80	−0.1 %
	NO_3^-	−1.00	−7.8 %	−0.07	0.6 %

results generally pass through the observations and to some extent, mirror their fluctuations (Fig. 3e–h). The NSE values for both NH_4^+ and NO_3^- during both calibration and validation periods range from −1.00 to 0.49, with the PBIAS varying from −23.1 % to 3.2 %. The low PBIAS values indicate that the simulation results do not exhibit significant bias. The NSE values may not appear high; however, it is regarded as acceptable, and even satisfactory, for the following two reasons. Firstly, "concentrations" rather than "loads" was used in evaluating model performance. Typically, when "loads" are utilized as the evaluation target, performance metrics (e.g., NSE) may appear more favorable due to streamflow weighting (Wellen et al., 2015). In this case, when calibrating the model based on "loads", the NSE values for NH_4^+ and NO_3^- range from 0.17 to 0.81, with the average NSE increased by 0.69 (Table S5 in the SM). We insist on using "concentrations" as the target is to focus on water quality simulation during the calibration process. Secondly, there may be notable errors in the PS inputs at the daily scale. As introduced in Section 2.3.1, PS inputs were estimated at an annual scale, and the model used corresponding averages in daily simulation. Although PS discharges are considered relatively stable, some input errors are inevitable.

Fig. 3 also indicates that the model performs well in the NRW but exhibits slightly poorer performance in the WRW. This can be attributed to the heightened impact of human activities in the WRW, which may not be accurately represented by the model (such as PS inputs). Furthermore, the observation process in the WRW, particularly at the QZ station, was significantly influenced by tidal fluctuations, leading to notable variations in the observations (Fig. 3f and h). Consequently, the simulation results appear to be less satisfactory. Additionally, the NO_3^- simulation outperforms the NH_4^+ simulation, primarily because NO_3^- simulation is predominantly influenced by NPS pollution, whereas NH_4^+ is primarily influenced by PS pollution, and the estimated PS inputs exhibit more significant uncertainty.

To further validate the model, simulated NH_4^+ and NO_3^- concentrations in surface runoff were compared with 20 concentration measurements observed at two stations in a subbasin of the JRW (Fig. S4 in the SM). Since NH_4^+ and NO_3^- concentrations in surface runoff can be directly influenced by local agricultural activities (e.g., fertilizer application), the time series of observed concentrations at the field scale may differ significantly from the simulated average concentrations at the HRU scale. Therefore, the comparison focuses on the variation in NH_4^+ and NO_3^- concentrations across different surface runoff events. As illustrated in Fig. S4, the simulated ranges of NH_4^+ and NO_3^- concentrations closely match the observed concentration ranges, thus validating the reliability of NH_4^+ and NO_3^- transport simulation to a certain degree.

The calibrated values of sensitive parameters for the NRW and WRW were presented in Table S3 in the SM. For the NRW, FRT_ADJ and PS_ADJ are calibrated to −0.199 and 0.192, respectively, close to their lower and upper limits. This suggests that the fertilization rates and PS loads for the NRW may be overestimated and underestimated, respectively. Conversely, in the case of the WRW, FRT_ADJ and PS_ADJ are calibrated to 0.199 and −0.199, indicating that the fertilization rates and PS loads may be underestimated and overestimated, respectively.

3.2. Sources and contributions of NH_4^+ pollution

3.2.1. NH_4^+ inputs

The total NH_4^+ input in the JRW was estimated to be 162,952 t N/a (~110 kg N/ha/a). NPS inputs are 153,753 t N/a (94.4 %), while PS inputs are 9199 t N/a (5.6 %). Fig. 4a and b summarize the NH_4^+ inputs in the NRW and WRW, respectively. The total inputs for these two watersheds are 60,345 and 91,667 t N/a, or 63 and 228 kg N/ha/a, respectively. The WRW received higher NH_4^+ input, primarily due to the more intensive agricultural practices in this region. Among the six nitrogen sources, fertilizer application is the predominant one, followed by atmospheric deposition. PS inputs primarily originated from livestock farming, as well as urban domestic sewage, collectively comprising over 90 % of the PS inputs in both watersheds. Detailed values for each NH_4^+ input source are provided in Table S6 in the SM. Notably, the correction effects of FRT_ADJ and PS_ADJ have been considered. Fig. S5 in the SM shows the annual PS and NPS NH_4^+ inputs during the simulation period. Generally, the NH_4^+ inputs are relatively stable, with a slight decrease trend in recent years.

3.2.2. Land-to-water delivery

While NPS inputs dominate the NH_4^+ inputs in the JRW, their contributions to NH_4^+ loads in streamflow remains unclear, regarding the strong retention effect of NH_4^+ by soil. To address this issue, we examined the movement of NH_4^+ in soil zone simulated by the modified SWAT. Fig. 5a summarizes the amounts of NH_4^+ leaving the soil zone via surface runoff, lateral flow, and percolation water. It is found that NH_4^+ primarily moves with surface runoff, constituting 84.1 % and 82.1 % of the total movement in the NRW and WRW, respectively. Lateral flow also carries a portion of NH_4^+, 15.8 % in the NRW and 17.4 % in the WRW. NH_4^+ in percolation water is minimal, only about 0.1 % and 0.5 % in the NRW and WRW, respectively. This result contrasts with the land-to-water process of NO_3^-, where a substantial portion of NO_3^- leaches into groundwater and subsequently reaches the rivers through return flow (Wang et al., 2024). Additionally, the minimal NH_4^+ leaching in the JRW does not imply that the groundwater simulation of NH_4^+ is unnecessary. Because, in some specific cases, such as artificial recharge of treated wastewater (Böhlke et al., 2006; Liu et al., 2023), NH_4^+ leaching can be significant. Dai et al. (2021) also found that NH_4^+ leaching in a karst watershed is very significant, leading to a reduction of NH_4^+ delivery to surface waters for about 36.9 %.

The above results indicate that the land-to-water delivery of NH_4^+ predominantly occurs through surface runoff and lateral flow. In the NRW, the delivery rate of NH_4^+ is 2260 t N/a, ~2.35 kg N/ha/a, and in the WRW, the delivery rate is 1164 t N/a, ~2.90 kg N/ha/a. Fig. 5b presents subbasin level NH_4^+ delivery rate for five land use categories (cropland, orchard & tea garden, grassland, forest, urban & other areas). The spatial variability of delivery rates is significant, ranging from 0.3 to 33 kg N/ha/a. Fig. 5c and d illustrate the distribution of delivery rates for these five categories in the NRW and WRW, respectively. It is observed that cropland and orchard & tea garden exhibit high delivery rates due to extensive fertilization, at 8.46 and 5.37 kg N/ha/a, respectively. In the WRW, orchard & tea garden show higher delivery rates, attributed to the extensive cultivation of pomelo, which has the highest fertilization rate (Fig. S2 in the SM). Grassland and forest, receiving no fertilizer, have low NH_4^+ delivery rates, at 1.29 and 1.19 kg N/ha/a, respectively. Delivery rates for urban & other areas are also significant, at 4.96 kg N/ha/a, primarily due to the presence of fertilization in these areas. Fig. 5 indicates that there could be significant difference in NH_4^+ delivery among different land uses due to varying NH_4^+ inputs. Even within the same land use, significant differences may

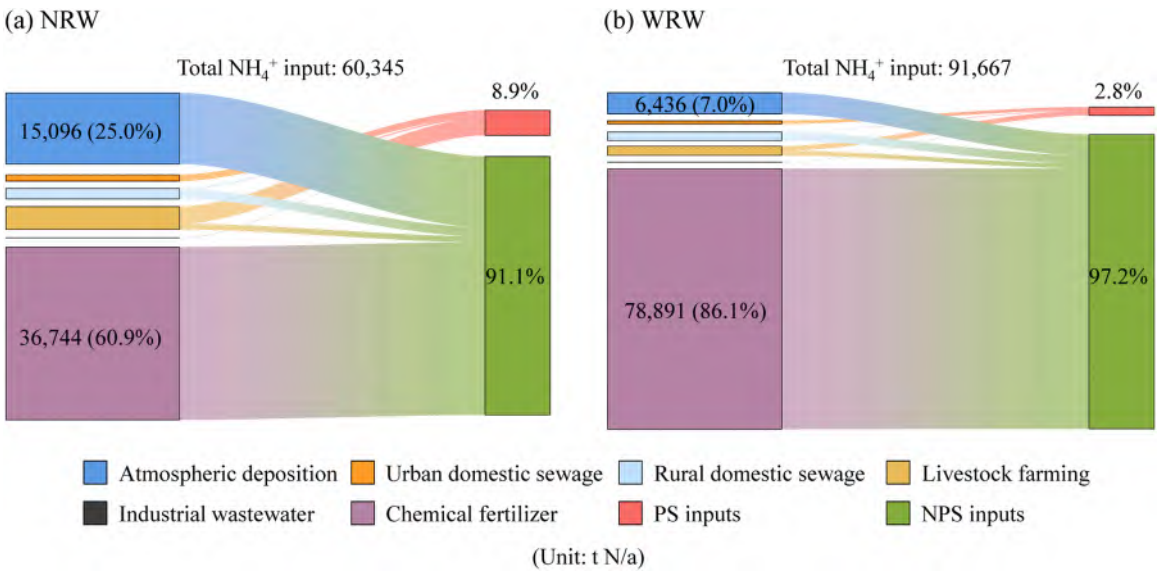

Fig. 4. NH_4^+ inputs in the North River Watershed (NRW) and West River Watershed (WRW). Subplots (a) and (b) are Sankey diagrams depicting NH_4^+ inputs from six sources in the NRW and WRW, respectively. PS and NPS represent point source and non-point source, respectively.

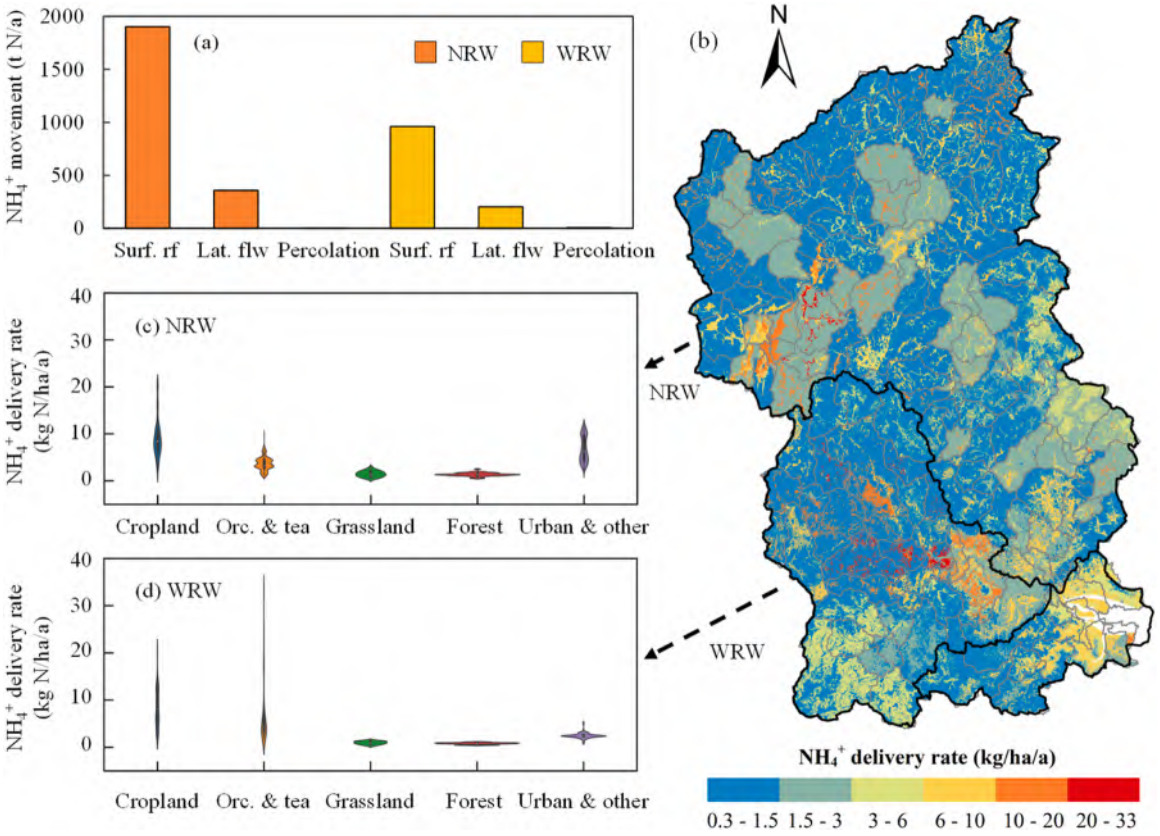

Fig. 5. NH_4^+ movement through surface runoff (surf. rf), lateral flow (lat. flw), and percolation water in the North River Watershed (NRW) and West River Watershed (WRW). Subplots b, c, and d summarize the delivery rate of NH_4^+ at the subbasin level for five land use categories. "Orc. & Tea" denotes "orchard and tea garden".

also exist due to the variations in soil properties, slope, precipitation, or even the timing of fertilization. This result highlights the necessity of employing WWQ models, such as SWAT, for spatially distributed simulation of NPS NH_4^+ processes. It is also worth noting that the JRW is a subtropical humid watershed. Therefore, the NH_4^+ delivery results from this study serve as a good reference for watersheds with similar climatic conditions.

3.2.3. *Contributions of PS and NPS NH_4^+ inputs*

As Fig. 6 shows, the NH_4^+ load in the baseline scenario (S0) is 1909 t N/a in the NRW and 2209 t N/a in the WRW. It can be decomposed into background load, PS-contributed load, NPS-contributed load, and an interactive impact between PS and NPS inputs. The background NH_4^+ load is 998 t N/a in the NRW and 686 t N/a in the WRW, accounting for 52.3 % and 31.0 % of the total load, respectively. The background load

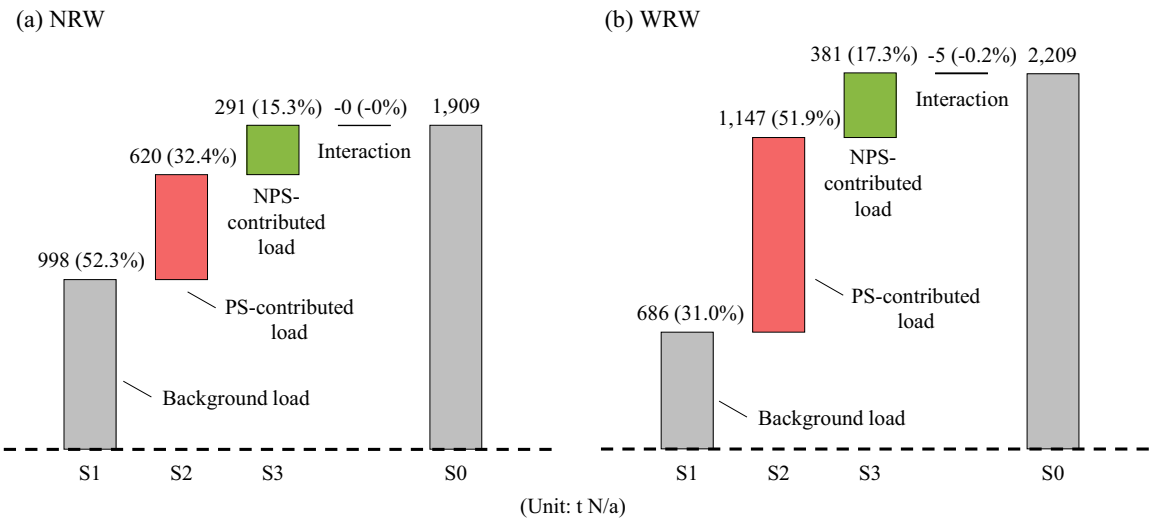

Fig. 6. Attribution of the NH_4^+ load at the outlets of (a) the North River Watershed (NRW) and (b) the West River Watershed (WRW) through scenario analysis. S1, S2, S3 and S0 represent four simulation scenarios (Section 2.4).

mainly originates from the hydrolysis of orgN in the streamflow. PS inputs contribute significantly, with 620 t N/a in the NRW (32.4 %) and 1147 t N/a in the WRW (51.9 %). This result indicates that controlling PS pollution is still the key to alleviate NH_4^+ pollution in the JRW. NPS inputs also play a role, contributing 291 t N/a of NH_4^+ in the NRW (15.3 %) and 381 t N/a in the WRW (17.3 %). This result underscores the importance of addressing NPS NH_4^+ processes in SWAT, which is overlooked. The interactive impact is minimal and can be disregarded.

Based on the above results, the in-stream NH_4^+ transport efficiencies in both the NRW and WRW can been estimated. Specifically, PS inputs and NPS loads (i.e., land-to-water loads) in the NRW amounted to 5534 and 2260 t N/a, resulting in corresponding NH_4^+ transport efficiencies of 0.116 and 0.129, respectively. In the WRW, the transport efficiencies for PS inputs and NPS loads were 0.454 and 0.327, respectively. This discrepancy can be attributed to the greater length of North River, where PS are mostly located upstream, affording NH_4^+ more time for oxidation into NO_3^-. In contrast, the shorter West River with PS closer to the outlet results in a smaller portion of NH_4^+ oxidation. This result reflects the complexity of simulating NH_4^+ at the watershed scale, given its susceptibility to oxidation, compared to the more stable NO_3^-.

3.3. *Management scenarios for the mitigation of NH_4^+ pollution*

As mentioned in Section 2.4, three measures were proposed for mitigating NH_4^+ pollution in the JRW. Fig. 7a and b show the reduction effects on NH_4^+ loads in the NRW and WRW when these measures were implemented individually (S4-S6) and collectively (S7). As shown, enhancing urban sewage treatment and improving livestock manure management can significantly reduce NH_4^+ load. Particularly in the WRW, these two measures have reduced NH_4^+ loads by 409 (18.5 %) and 321 (14.5 %) t N/a, respectively. Reducing chemical fertilizer has also led to a slight decrease in NH_4^+ pollution, with reductions of 48 (2.5 %) and 88 (4 %) t N/a in the NRW and WRW, respectively. When the three measures are implemented simultaneously, the NRW experiences a reduction of 452 (23.7 %) t N/a in NH_4^+ load, and the WRW exhibits a reduction of 818 (37 %) t N/a. These results indicate that the three measures are effective in reducing the NH_4^+ load in the JRW.

Compared with the "loads", managers may be more concerned about whether the "concentrations" meet the standards. Fig. 7c presents the simulated NH_4^+ concentrations at the outlet of the NRW under Scenarios S0 and S7. NH_4^+ concentrations in Scenario S0 show a decreasing trend over time. This is mainly attributed to the continuous improvement in treatment levels of PS pollution. The simulation differences between Scenarios S0 and S7 also decrease over time, mainly because the PS pollution treatment levels in Scenario S0 already approach the enhanced measures in Scenario S7 in the later stages of the simulation period (particularly since 2016). Notable seasonal fluctuations were observed, with high concentrations mainly occurring during the winter (i.e., low-flow periods). This result suggests that managers should particularly emphasize PS pollution control in winter.

Furthermore, we evaluated the water quality at the outlet using China's surface water quality standards (SEPA 2002). Based on NH_4^+ concentration, the water quality at the outlet was categorized into four classes: Class I ($\leq$0.15 mg N/L), Class II ($\leq$0.5 mg N/L), Class III ($\leq$1 mg N/L), and Class >III (>1 mg N/L). The classification of waters into Classes I, II and III is not mutually exclusive, but compatible. For example, a concentration of 0.1 mg N/L will be classified as Class I, as well as Classes II and III. This classification method, not a typical management practice, is solely used to facilitate assessing water quality improvements. By examining daily concentrations, we calculated the frequency of each class in both scenarios (Fig. 7d). The three measures resulted in increased frequencies of water quality falling into Classes I, II, and III. Particularly, the Class II frequency increased from 0.79 to 0.95. Fig. 7e and f illustrate the results for the WRW. The NH_4^+ concentrations in the WRW are higher than those in the NRW, indicating a more severe pollution situation. The mitigation effects of the three measures are quite significant, with the Class III frequency increasing from 0.64 to 0.92.

4. Discussions

The NH_4^+ simulation method developed in this study is specifically designed for permeable areas within the watershed. In impervious urban areas, the SWAT model only simulates NO_3^- and orgN, despite certain experimental studies indicating that NH_4^+ dominates the composition of total nitrogen in urban runoff (Wang et al., 2022). We refrained from modifying the urban simulation process primarily due to the lack of data for improving the model. Additionally, the contribution of NH_4^+ from impervious areas is negligible in the JRW. However, when simulating highly urbanized watersheds, careful consideration should be given to the simulation of NH_4^+ pollution in urban runoff.

The modeling experience in the JRW emphasizes that simulating NH_4^+ at the watershed scale is more challenging compared with the relatively stable NO_3^-. Traditionally, in the model setup process, NO_3^- simulations primarily focus on the total input of mineral nitrogen, neglecting the distinction between NH_4^+ and NO_3^- input, as NH_4^+ can be

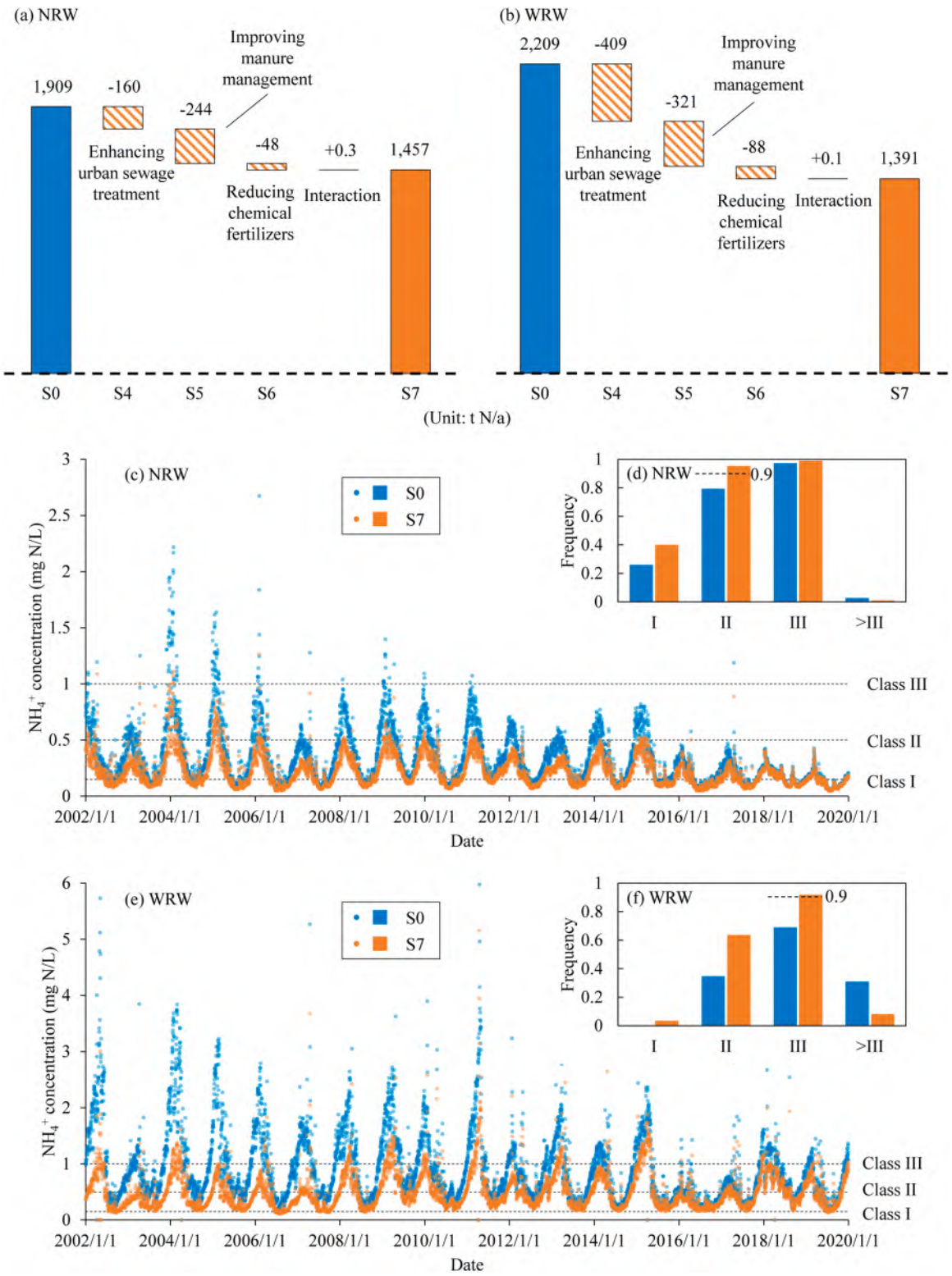

Fig. 7. NH_4^+ simulation results for the baseline scenario (S0) and several management scenarios (S4-S7). Subplots a and b illustrate the effect of proposed measures in reducing NH_4^+ loads within the North River Watershed (NRW) and West River Watershed (WRW), respectively. Subplots c and e show the simulated NH_4^+ concentrations at the outlets of NRW and WRW, respectively. Subplots d and f show the frequencies of water quality classifications for the NRW and WRW, respectively. Concentration thresholds for Classes I, II and III are 0.15, 0.5 and 1 mg N/L, respectively.

rapidly nitrified into NO_3^-. However, in NH_4^+-targeted simulations, precise estimation of NH_4^+ input is crucial. Considering the transformation relationship between NH_4^+ and NO_3^-, it is necessary to simultaneously calibrate NO_3^- when calibrating NH_4^+. NO_3^- observations can assist in constraining the oxidation of NH_4^+, potentially enhancing the reliability of the model. In addition to NO_3^-, streamflow should also be calibrated, which provide reasonable hydrological driving for water quality simulations. Other relevant model responses, such as sediment, leaf area index, etc., can also be considered in the calibration process. Our previous research demonstrated that multi-response calibration can

improve the reliability of simulation results (Han and Zheng 2016).

The source-contribution analysis demonstrates that PS pollution plays a crucial role in NH_4^+ pollution in the JRW. This finding indicates that the control of PS pollution, such as domestic sewage and livestock farming discharges, remains a priority in NH_4^+ pollution mitigation. It also suggests that modelers should pay more attention to the collection and assessment of PS pollution data, which has been simplified or overlooked. NPS pollution also plays a role in NH_4^+ pollution. By implementing measures such as near-channel management (Hansen et al., 2021) and reduction of fertilization rate, it is possible to reduce NH_4^+ pollution to a certain extent. Given that NH_4^+ primarily moves with surface runoff and lateral flow, efforts to control NPS pollution should be concentrated during precipitation periods. For example, no fertilization during rainy days could be a viable approach. Additionally, a significant portion of the NH_4^+ in rivers originates from the hydrolysis of orgN, making the reduction of orgN from PS and NPS another potential solution for NH_4^+ mitigation.

In real-world management, a series of candidate NH_4^+ mitigation measures should be initially designed, based on the watershed's pollution sources and their contributions. Then, appropriate mitigation measures can be selected through cost-effectiveness optimization (Ahmadi et al., 2013; Hansen et al., 2021). WWQ models can serve as effective decision-support tools. In this regard, ensuring the precise representation of these measures in the model and considering their inherent uncertainty in optimization are crucial for making effective decisions (Dai et al., 2018). Note that this study mainly focuses on evaluating the effectiveness of measures rather than implementing a complete decision-making process, so we didn't systematically evaluate the cost of the three proposed measures.

5. Conclusions

In this study, the classical SWAT model was enhanced to simulate NPS NH_4^+ processes. The modification is process-based, specifically incorporating the simulation of land-to-water NH_4^+ delivery. The modified model was applied to the JRW, a coastal watershed with significant anthropogenic nitrogen inputs. The model was well calibrated, and the simulation results are deemed satisfactory. The study examined NPS NH_4^+ processes, identified key NH_4^+ sources, quantified their contributions to in-stream loads, and evaluated several pollution mitigation measures. The main findings of this study are as follows:

- The modified SWAT model can effectively simulate the NPS NH_4^+ pollution processes. The inherent instability of NH_4^+ makes it challenging to calibrate NH_4^+ simulation. It is recommended to use multiple sets of observations, especially NO_3^-, to calibrate the model to enhance model reliability.
- NPS inputs dominate the NH_4^+ input in the JRW (94.4 %), but PS inputs makes a more significant contribution to the NH_4^+ load at watershed outlet. Specifically, PS inputs contributes 32.4 % and 51.9 % to the NH_4^+ load in the NRW and WRW, respectively, while NPS inputs contribute 15.3 % and 17.3 %, respectively. The remaining load originates from the hydrolysis of orgN.
- NH_4^+ primarily enters water through surface runoff (83.4 %) and lateral flow (16.3 %). NH_4^+ leaching into groundwater (0.2 %) is negligible. Average NH_4^+ delivery rates in the NRW and WRW are 2.35 and 2.90 kg N/ha/a, respectively. The delivery rate exhibits significant spatial heterogeneity, from 0.3 to 33 kg N/ha/a. High delivery areas primarily occur at agricultural areas.
- Three NH_4^+ mitigation measures, i.e., enhancing urban sewage treatment, improving livestock manure management, and reducing fertilizer application, were proposed and evaluated. These measures can collectively reduce approximately 1/4 and 1/3 of the NH_4^+ load in the NRW and WRW, respectively. They also raise the frequencies of the North River and West River meeting Class II and Class III water quality standards to over 90 %, respectively.

CRediT authorship contribution statement

Feng Han: Conceptualization, Methodology, Software, Writing – original draft, Writing – review & editing. **Qing Tian:** Data curation, Formal analysis, Investigation. **Nengwang Chen:** Data curation, Funding acquisition, Supervision, Writing – review & editing. **Zhaoping Hu:** Investigation, Software. **Yao Wang:** Data curation, Formal analysis, Validation. **Rui Xiong:** Validation, Visualization. **Peng Xu:** Formal analysis, Validation. **Wei Liu:** Investigation, Formal analysis. **Alejandra Stehr:** Validation, Writing – review & editing. **Ricardo O. Barra:** Validation, Writing – review & editing. **Yi Zheng:** Funding acquisition, Methodology, Supervision, Validation, Writing – review & editing.

Declaration of competing interest

The authors declare that they have no known competing financial interests or personal relationships that could have appeared to influence the work reported in this paper.

Data availability

Data will be made available on request.

Acknowledgements

This study is supported by the National Natural Science Foundation of China (NSFC) (No. 51961125203; No. 41676098), Shenzhen Science and Technology Innovation Commission (No. KCXFZ202002011006491), and the Fujian Province Water Conservancy Science and Technology Project (No. MSK202301; No. MSK202313). Additional support is provided by the State Environmental Protection Key Laboratory of Integrated Surface Water-Groundwater Pollution Control. We thank all the students for their assistance in observation and laboratory analysis.

Supplementary materials

Supplementary material associated with this article can be found, in the online version, at doi:10.1016/j.watres.2024.121372.

References

Ahmadi, M., Arabi, M., Hoag, D.L., Engel, B.A., 2013. A mixed discrete-continuous variable multiobjective genetic algorithm for targeted implementation of nonpoint source pollution control practices. Water. Resour. Res. 49 (12), 8344–8356.
Althoff, D., Rodrigues, L.N., 2021. Goodness-of-fit criteria for hydrological models: model calibration and performance assessment. J. Hydrol. 600, 126674.
Ao, C., Yang, P., Zeng, W., Jiang, Y., Chen, H., Xing, W., Zha, Y., Wu, J., Huang, J., 2020. Development of an ammonia nitrogen transport model from surface soil to runoff via raindrop splashing. Catena 189, 104473.
Bicknell, B.R., Imhoff, J.C., Kittle, J.J.L., Donigian, J.A.S., Johanson, R.C., 1997. Hydrological Simulation Program – FORTRAN, User's Manual For Version 11. U.S. Environmental Protection Agency.
Bingner, R.L., Theurer, F.D., Yuan, Y., 2018. AnnAGNPS Technical Processes: Version 5.5. USDA-ARS National Sedimentation Laboratory.
Böhlke, J.K., Smith, R.L., Miller, D.N., 2006. Ammonium transport and reaction in contaminated groundwater: application of isotope tracers and isotope fractionation studies. Water. Resour. Res. 42 (5), W05411.
Campolongo, F., Cariboni, J., Saltelli, A., 2007. An effective screening design for sensitivity analysis of large models. Environ. Modell. Softw. 22 (10), 1509–1518.
Chen, B., Wang, K., Dong, X., Lin, H., 2021. Long-term changes in red tide outbreaks in Xiamen Bay in China from 1986 to 2017. Estuar. Coast. Shelf. Sci. 249, 107095.
Dai, C., Qin, X.S., Tan, Q., Guo, H.C., 2018. Optimizing best management practices for nutrient pollution control in a lake watershed under uncertainty. Ecol. Indic. 92, 288–300.
Dai, Y., Lang, Y., Wang, T., Han, X., Wang, L., Zhong, J., 2021. Modelling the sources and transport of ammonium nitrogen with the SPARROW model: a case study in a karst basin. J. Hydrol. 592, 125763.
Daniels, S.M., Evans, M.G., Agnew, C.T., Allott, T.E., 2012. Ammonium release from a blanket peatland into headwater stream systems. Environ. Pollut. 163, 261–272.

Delgrosso, S., Mosier, A., Parton, W., Ojima, D, 2005. DAYCENT model analysis of past and contemporary soil N2O and net greenhouse gas flux for major crops in the USA. Soil Tillage Res. 83 (1), 9–24.
Ding, S., Dan, S.F., Liu, Y., He, J., Zhu, D., Jiao, L., 2022. Importance of ammonia nitrogen potentially released from sediments to the development of eutrophication in a plateau lake. Environ. Pollut. 305, 119275.
EA, 2005. Development of the Partition Coefficient (Kd) Test Method For Use in Environmental Risk Assessments. Environment Agency, Bristol, England.
Fu, B., Merritt, W.S., Croke, B.F.W., Weber, T.R., Jakeman, A.J., 2019. A review of catchment-scale water quality and erosion models and a synthesis of future prospects. Environ. Modell. Softw. 114, 75–97.
Gu, B., Zhang, X., Lam, S.K., Yu, Y., van Grinsven, H.J.M., Zhang, S., Wang, X., Bodirsky, B.L., Wang, S., Duan, J., Ren, C., Bouwman, L., de Vries, W., Xu, J., Sutton, M.A., Chen, D, 2023. Cost-effective mitigation of nitrogen pollution from global croplands. Nature 613, 77–84.
Han, F., Zheng, Y., 2016. Multiple-response Bayesian calibration of watershed water quality models with significant input and model structure errors. Adv. Water. Resour. 88, 109–123.
Hansen, A.T., Campbell, T., Cho, S.J., Czuba, J.A., Dalzell, B.J., Dolph, C.L., Hawthorne, P.L., Rabotyagov, S., Lang, Z., Kumarasamy, K., Belmont, P., Finlay, J. C., Foufoula-Georgiou, E., Gran, K.B., Kling, C.L., Wilcock, P., 2021. Integrated assessment modeling reveals near-channel management as cost-effective to improve water quality in agricultural watersheds. Proc. Natl. Acad. Sci. 118 (28), e2024912118.
Jia, Y., Wang, Q., Zhu, J., Chen, Z., He, N., Yu, G., 2019. A spatial and temporal dataset of atmospheric inorganic nitrogen wet deposition in China (1996-2015). Sci. Data Bank 4 (1).
Jia, Y., Wang, Q., Zhu, J., Chen, Z., He, N., Yu, G., 2021. A spatial and temporal dataset of atmospheric inorganic nitrogen dry deposition in China (2006-2015). Sci. Data Bank 6 (2).
Jiang, J., Wang, Z., Lai, C., Wu, X., Chen, X., 2023. Climate and landuse change enhance spatio-temporal variability of Dongjiang river flow and ammonia nitrogen. Sci. Total Environ. 867, 161483.
Kong, H., Lin, H., Peng, B., Chen, N., Lin, C., Fielding, S., 2015. Modelling the cost-effective solutions of nitrogen reduction in Jiulong River Watershed, China. Estuar. Coast. Shelf Sci. 166, 218–229.
Liu, J., Yuan, J., Zhang, Y., Zhang, H., Luo, Y., Su, Y., 2023. Identification of ammonium source for groundwater in the piedmont zone with strong runoff of the Hohhot Basin based on nitrogen isotope. Sci. Total Environ. 882, 163650.
Luo, Y., Liu, J.W., Wu, J.W., Yuan, Z., Zhang, J.W., Gao, C., Lin, Z.Y., 2022. Comprehensive assessment of eutrophication in Xiamen Bay and its implications for management strategy in southeast China. Int. J. Environ. Res. Public Health 19 (20), 13055.
MEE, 2020. The Second National Census of Pollution Sources. Ministry of Ecology and Environment of China.
Moriasi, D.N., Arnold, J.G., Liew, M.W.V., Bingner, R.L., Harmel, R.D., Veith, T.L., 2007. Model evaluation guidelines for systematic quantification of accuracy in watershed simulations. Trans. ASABe 50 (3), 885–900.
Morris, M.D., 1991. Factorial sampling plans for preliminary computational experiments. Technometrics 33 (2), 161–174.
Neitsch, S.L., Arnold, J.G., Kiniry, J.R., Williams, J.R., 2011. Soil and Water Assessment Tool: Theoretical Documentation Version 2009. Texas Water Resources Institute.
O'Mara, K., Olley, J.M., Fry, B., Burford, M., 2019. Catchment soils supply ammonium to the coastal zone - Flood impacts on nutrient flux in estuaries. Sci. Total Environ. 654, 583–592.
Regis, R.G., Shoemaker, C.A., 2013. Combining radial basis function surrogates and dynamic coordinate search in high-dimensional expensive black-box optimization. Eng. Optim. 45 (5), 529–555.
Saxton, K.E., Willey, P.H., 2005. The SPAW model for agricultural field and pond hydrologic simulation. In: Singh, V.P., Frevert, D.K. (Eds.), Watershed models. CRC Press, Boca Raton, pp. 400–435.
Schimel, J.P., Bennett, J., 2004. Nitrogen mineralization: challenges of a changing paradigm. Ecology. 85 (3), 591–602.
Schwarz, G., Hoos, A., Alexander, R., Smith, R., 2006. The SPARROW Surface Water Quality Model: Theory, Application and User Documentation. U.S. Geological Survey.
SEPA, 2002. Environmental Quality Standards for Surface Water (GB 3838-2002). State Environmental Protection Administration of China.
UNH-ISEOS, 2017. DNDC (version 9.5): Scientific Basis and Processes. Institute for the Study of Earth, Oceans, and Space, University of New Hampshire, Durham, USA.
Vaighan, A.A., Talebbeydokhti, N., Bavani, A.M., Whitehead, P., 2019. Modeling impacts of climate and land use change on streamflow, nitrate, and ammonium in the Kor River, southwest of Iran. J. Water. Clim. Chang. 10 (4), 818–834.
Wade, A.J., Durand, P., Beaujouan, V., Wessel, W.W., Raat, K.J., Whitehead, P.G., Butterfield, D., Rankinen, K., Lepisto, A., 2002. A nitrogen model for European catchments: INCA, new model structure and equations. Hydrol. Earth. Syst. Sci. 6 (3), 559–582.
Wang, S., Ma, Y., Zhang, X., Shen, Z., 2022. Transport and sources of nitrogen in stormwater runoff at the urban catchment scale. Sci. Total Environ. 806, 150281.
Wang, Y., Yu, Y., Luo, X., Tan, Q., Fu, Y., Zheng, C., Wang, D., Chen, N., 2024. Prioritizing ecological restoration in hydrologically sensitive areas to improve groundwater quality. Water Res. 252, 121247.
Wellen, C., Kamran-Disfani, A.R., Arhonditsis, G.B., 2015. Evaluation of the current state of distributed watershed nutrient water quality modeling. Environ. Sci. Technol. 49 (6), 3278–3290.
Xing, W., Sun, G., Zou, Z., Li, Y., Yang, P., Ao, C., 2023. Mathematical model of ammonia nitrogen transport from soil to runoff on irregular slopes. J. Hydrol. 620, 129440.
Xu, P., Li, G., Zheng, Y., Fung, J.C.H., Chen, A., Zeng, Z., Shen, H., Hu, M., Mao, J., Zheng, Y., Cui, X., Guo, Z., Chen, Y., Feng, L., He, S., Zhang, X., Lau, A.K.H., Tao, S., Houlton, B.Z., 2024. Fertilizer management for global ammonia emission reduction. Nature 626, 792–798.
Yang, J., Reichert, P., Abbaspour, K.C., Yang, H., 2007. Hydrological modelling of the Chaohe Basin in China: statistical model formulation and Bayesian inference. J. Hydrol. 340 (3–4), 167–182.
Yu, C., Huang, X., Chen, H., Godfray, H.C.J., Wright, J.S., Hall, J.W., Gong, P., Ni, S., Qiao, S., Huang, G., Xiao, Y., Zhang, J., Feng, Z., Ju, X., Ciais, P., Stenseth, N.C., Hessen, D.O., Sun, Z., Yu, L., Cai, W., Fu, H., Huang, X., Zhang, C., Liu, H., Taylor, J., 2019. Managing nitrogen to restore water quality in China. Nature 567, 516–520.
Zaidi Farouk, M.I.H., Jamil, Z., Abdul Latip, M.F., 2023. Towards online surface water quality monitoring technology: a review. Environ. Res. 238, 117147.
Zhang, H., Cao, X., Huo, S., Ma, C., Li, W., Liu, Y., Tong, Y., Wu, F., 2023. Changes in China's river water quality since 1980: management implications from sustainable development. NPJ. Clean. Water. 6 (45).
Zhang, X., Zou, T., Lassaletta, L., Mueller, N.D., Tubiello, F.N., Lisk, M.D., Lu, C., Conant, R.T., Dorich, C.D., Gerber, J., Tian, H., Bruulsema, T., Maaz, T.M., Nishina, K., Bodirsky, B.L., Popp, A., Bouwman, L., Beusen, A., Chang, J., Havlik, P., Leclere, D., Canadell, J.G., Jackson, R.B., Heffer, P., Wanner, N., Zhang, W., Davidson, E.A., 2021. Quantification of global and national nitrogen budgets for crop production. Nat. Food 2 (7), 529–540.
Zhou, Q., Gao, J., Zhang, R., Zhang, R., 2017. Ammonia stress on nitrogen metabolism in tolerant aquatic plant-Myriophyllum aquaticum. Ecotoxicol. Environ. Saf. 143, 102–110.
Zhu, D., Cheng, X., Li, W., Niu, F., Nayeb Yazdi, M., 2023. Estimating the impact of temperature and streamflow change on river nitrogen pollution using the land-river integrated modeling system. J. Hydrol. 626, 130190.